

On the Review of Dehazing Methods for Bad Weather Images

R. Suganya^{*}, Dr.R. Kanagavalli[#]

Department of Computer Science and Engineering^{*}, Department of Information Science and Engineering[#]
New Horizon College of Engineering^{*}, The Oxford College of Engineering[#]
Bengaluru, India

Abstract — This paper reports the collective review on the proposals from the literatures related to image enhancement in outdoor scenes. Images captured in natural environment are subject to bad weather conditions including haze, mist and fog which would spoil the appearance of images. Edge, contrast and brightness are the features usually affected in an image because the fog pixels blur total scene and spoil the edges. Since the quality of images is ruined, they turn to be useless for any type of evaluation. This problem is very serious in online applications not limited to driving assistance, satellite imageries and defense applications. Therefore, a thorough conceptual study on all the existing methods to mitigate the haze in the images had been presented in this paper. Results from earlier works were compared based on the Peak Signal to Noise ratio, Structural Similarity index metric, Percentage of saturated pixels, Visible Edges ratio, and Perceptual haze density metrics. Ultimately, few suggestions to improve the dehazing performance have been presented.

Keywords — Image enhancement, Fog removal, driving assistance, chaos and Road traffic images

I. INTRODUCTION

Acquiring indoor images is pretty simple and mostly does not involve any post processing. The same is very critical in outdoor imaging, since the light from the scene element is scattered due to natural or artificial light sources. So, quality of images acquired at outdoor is highly dependent on atmospheric conditions. Moreover, the variation in contrast is an exponential decay through the depth of the image. Prevailing intelligent methods for surveillance, recognition, navigation and classification based on image processing exist at the mercy of quality features hidden in an image. Hence, it is vital to enhance the images prior to using the images for needy applications.

This survey is envisioned to present the existing enhancement algorithms in spatial domain, time domain and frequency domain along with its strengths and weaknesses. Of course, enhancement would mean any one or all of the parameters such as; Brightness, Contrast, Color, Edges, Blur etc. It is widely seen that the researchers had focused on appropriate algorithms only to specific applications to enhance the image content. Nonetheless, most of the dehazing algorithms

contain the sequence as mentioned in Fig. 1. The steps include depth map estimation, atmospheric light and transmission map estimation, refinement of depth map, restoration model estimation and recovery of haze free image.

This review paper has been organized as follows. Section II presents clear picture on how the images are degraded based on the atmospheric conditions. Section III offers discussion on existing popular dehazing algorithms along with merits and demerits observed on those research works. Section IV narrates the metrics conventionally used in de-hazing algorithms along with newly proposed metrics. Section V gives a conclusive remarks and future enhancements to be carried out.

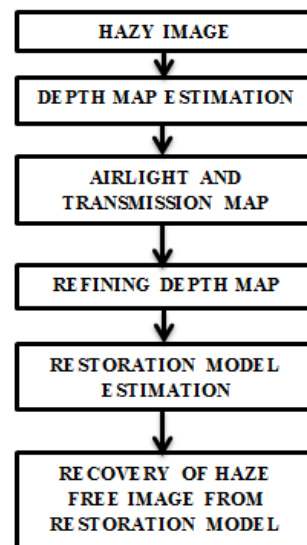


Fig. 1 Sequence of dehazing operations

II. IMAGE DEGRADATION MODEL

A. Origin of image degradation

Prior to disclose the image degradation model, it is essential to review the source atmospheric conditions responsible for degradation. There exist two poor weather conditions: Steady and Dynamic conditions [1]. Haze, fog and mist are caused due to the atmospheric particle of sizes 1-10 μ m. The case is

still severe due to rain and snow where the particle sizes are in the range of 1-100 μ.m for moderate rains [2]. The illumination effect at a pixel of interest is bound to the atmospheric particle or rain droplets within the solid angle of the pixel.

Table 1 Particle size variation

Poor Weather condition	Environments	Particle size (μm)
Static	Haze, Fog, Mist	1-10
Dynamic	Rain, Snow	1-100

As seen in Fig. 2, the light received by the imaging system is an integrated effect of light from the scene element and the illumination from natural or artificial source. Since the atmospheric particles exist between the camera and the scene, they tend to scatter the light in various directions. Hence, the intensity of light reaching the camera decays exponentially as the scene depth increases [3].

Road traffic images, underwater images, natural scene images are prone to acquire more haze effects than the indoor images.

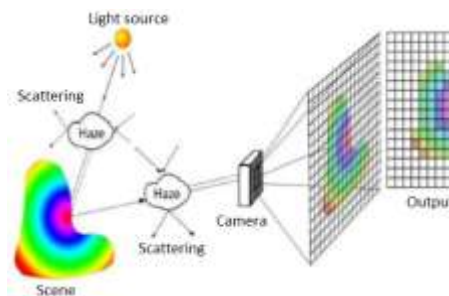


Fig. 2 Outdoor image capturing phenomena

B. Scene Depth Estimation

The following are the models seen in earlier literatures

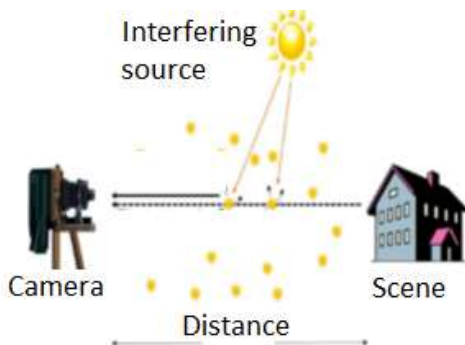


Fig. 3 Scattering mechanism

$$I_{mg}(k) = J_{sr}(k) M_{tx}(k) + G_{al}(1 - M_{tx}(k)) \quad (1)$$

Where, I_{mg} is the intensity of the image as seen by the viewer, J_{sr} indicates the radiance of the scene, k represents the position of the pixel and G_{al} points out the global atmospheric light. M_{tx} specifies diminishing portion of light reaching observing point, whose magnitude is an exponential decline, based on the distance between the observing point and the scene point as given in Equation (2). This is called as transmission map.

$$M_{tx}(k) = e^{-\beta d(k)} \quad (2)$$

Where, β is the scattering coefficient and d is the distance between the scene and the camera at pixel location k .

Of course, this portion of light is not scattered by any external particles and reaches the camera directly [4]. This mathematical formulation is usually agreed for the digital images captured from natural outdoor scenes. It is apparent that the concept behind the removal of haze is to obtain J_{sr} from perceived image intensity I_{mg} , estimated atmospheric light G_{al} and transmission map M_{tx} . Equation (1) shown above is popularly understood as Koschmiedar’s Law as given in [5], [6] and [7].

In [4], Fattal introduced an enhanced mathematical model to describe the formation of image using parameter namely, surface albedo (S_{ac}). The term J_{sr} is replaced with $S_{ac} \times S_f$ where, S_{ac} is related to amount of light reflected from a surface given by the ratio of radiant flux leaving the surface to the irradiance [62],[63] and S_f is the shading factor. In this model, difficulties experienced in conventional single image de-hazing methods have been overcome by solving for shading and transmission functions. The same principle is used to estimate the atmospheric light also.

It is difficult to estimate the amount of light absorbed in the medium and the depth of the observed scene. However, these parameters highly affect the transmission M_{tx} . Therefore, an alternate method is found where atmospheric veil $A_{veil}(k) = G_{al}(1 - M_{tx}(k))$ was introduced. Therefore, mathematical model to form an image is rewritten as follows

$$I_{mg}(k) = J_{sr}(k) \left(1 - \frac{A_{veil}(k)}{G_{al}}\right) + A_{veil}(k) \quad (3)$$

In [39], prior to perform visibility restoration, white balance was initially done by replacing the pixels with local image averages after the observed image I_{mg} was normalized. Therefore, in Equation (4), $A_{veil}(k)$ is essential instead of M_{tx} for image enhancement.

In [8], estimation of transmission M_{tx} and atmospheric light G_{al} is done based on evaluating the Dark Channel Prior (DCP). The parameter DCP is

calculated using the pixels whose gray levels are near to zero or typically zero in at least any one the color layers R, G, and B in the haze free images. The DCP J_{dc} is estimated using two minimum commutative operators as follows.

$$J_{dc} = \min_{z \in O(k)} (\min_{cc \in RGB} (J_{sr}^{cc})) \quad (4)$$

Where, cc in Equation (4) is a color layer of J_{sr} and $O(k)$ is a local region centered at k .

In [9], scene depth $I_{depth}(k)$ was estimated using Color Attenuation prior (CAP) while discarding the transmission $M_{tx}(k)$, by Zhu et al. A linear relationship was constructed with scene brightness $S_b(k)$, saturation $I_{st}(k)$ and random error likely to be added as given below.

$$I_{depth}(k) = LC_0 + LC_1 S_b(k) + LC_2 I_{st}(k) + R_r(k) \quad (5)$$

Where, LC_0 , LC_1 and LC_2 are three unknown linear coefficients chosen to be 0.12, 0.95 and 0.78 respectively obtained using maximum likelihood based supervised learning method. R_r is the random error with a Gaussian density, which gives $R_r(k) \in N(0, \sigma^2)$. Furthermore, 500 haze-free images were used in [9] as the training samples to estimate the constants in the Equation (5) along with mean of the normal distribution, $\mu = 0.04$.

C. Transmission Map Estimation

As mentioned in [10], it is good to propose appropriate priors to evaluate the transmission map to obtain the haze free image. Three types of prior are seen: similarity prior, local prior and global prior.

Though Similarity prior is popular, it is inaccurate due to its dependency on dictionary model created using sample images using data driven hypothesis [11]-[16]. Similarity prior resulted in reconstruction defects due to unrealistic extension of scene structure.

Global prior had attracted the research community due to its stringent mathematical base. As the name specifies, this type of prior is calculated for the whole of the image instead of local region in an image. This approach is divided into two groups. The first group relies on the method of assuming the image to be a continuous function space with an ability to measure the global regulatory. Dehazing algorithms emerged out of this prior uses a total variation minimization [17]. The second group of global prior is related to statistical distribution. This approach had been used in [18], where Bayesian statistical prior estimated both albedo and depth from a single frame. However, the result was an over enhancement. Similarly, [9] was also not compromising due to large depth jumps, when global color attenuation prior was used.

While observing the global and similarity prior, it is transparent that poor results are due to the negligence of the local features. Anyhow, works in

[19] also resulted in over enhancement and look unnatural while using the local features. Researchers in [4] and [20] modeled the pixels of a haze image as a Markov Random Field (MRF) while applying the planar constraints. Similar work had been done in [21] where depth estimation was done using fusion method. The problem was handled as minimization of local energy where the variables have dependencies based on Spatial Markov model. It is common in image processing to make use of filters to remove the unwanted frequency bands. Such filtering approaches had been done in [22]-[24] to calculate the transmission map. He et al, in [8] offered an efficient enhancement through improved evaluation of transmission map for open-air colored RGB images. Among all the aforementioned techniques, the Dark Channel Prior ranked top. Authors of [25], [26] used a local prior to estimate a depth propagation framework for circumstances in which the dark channel prior was ambiguous. A simplified dark channel prior, lowest level channel prior had been used in [27]. But, the result was halo artifacts especially for neighbors of edge pixels when min filter was used. Hence, bilateral filter was used to solve the problem.

D. Depth Map Refinement

Refining the depth map reference is governed by Equation (6)

$$\overline{M_{tx}} = 1 - \frac{A_{veil}}{G_{al}^{cc}} \quad (6)$$

Where,

$$G_{al} = \max_{z \in I_{mg}} (\min_{z \in O(k)} (I_z^{cc})) \quad (7)$$

E. Restoring the original scene image

Restoring the original scene in the image is done based on the following Equation (8).

$$J_{sr}(k) = \frac{I_{mg}(k) - G_{al}}{\max(M_{tx}(k), L_b)} + G_{al} \quad (8)$$

III. EXISTING DEHAZING ALGORITHMS

Research works done in [28]-[32] focused on contrast restoration but required multi temporal images. This would not be suitable for real time applications, because real time applications would not have the original scene images.

Reference [33] had used simple fusion method to obtain a better image. Multiple images of same scene were fused in wavelet domain and finally performed the inverse wavelet transforms. Anyhow, the method failed to account the amount of scattering due to which the image had been degraded. Narasimhan & Nayar in [34], proposed a dichromatic atmospheric scattering model. Based on this model, color deviations in the image subject to dissimilar weather conditions were observed as given in [35]. Clear day scene colors were estimated by computing 3D structure from two or more bad images [36]. Anyhow, the major drawback is their negligence on the atmospheric scattering properties due to change in

wavelength of light. Additional problem is ambiguous scene points when it matches with color of fog. Due to this, scene pixels will be removed along with fog pixels. Narasimhan & Nayar in [37] presented a physic based model that could describe well the scene structure. This method never needed any a-priori scene structure and specific knowledge on weather conditions. However, structure computation required two images with similar daylight spectra but with different weather conditions.

Works done in [38] reports on the evaluation of the weather conditions and obtained an approximate three dimensional geometrical view of the image scene, which is given a-priori and further refined during the restoration process. Though [39] had implemented faster algorithm for real time applications, it could not differentiate white objects and the fog.

A method of fog estimation was done in [40] to eliminate the visibility loss in camera based driver assistance systems. Then, contrast was restored using flat-world assumption on the segmented free space for the road scene shown in Fig. 4. Based on efficient 3D estimation, Road marking, Road sign extraction and Road obstacle detection had been tested on real time images instead of synthetic images. However, this work could not handle all road traffic scenes.

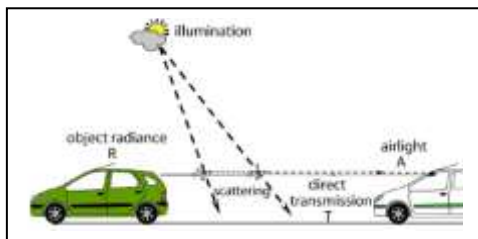


Fig. 4 Road traffic scene

Anisotropic diffusion based fog removal was attempted in [41]. The first mathematical model based on non-linear anisotropic diffusion was introduced by Perona & Malik in [42]. In this method, image content is selectively smoothed with a primary task of edge protection. The whole of the diffusion process is well governed by the partial differential equation (PDE). The algorithm was valid for grey and color images. It was found that the computation time was reduced further while HSI (Hue, Saturation and Intensity) model images were tested. The outcome of the research was found to be independent of fog density and user. The simulation results could be compatible with prior state-of-the-art algorithms based on contrast gain, computation time and percentage of saturated pixels [43].

Reference [44] introduced a concept of transmission map in modified version. Multiphase level set formulation was used to generate the map. Furthermore, ambient light intensity was also

measured. The method could preserve the color in consecutive video frames based on the temporal difference ratio of HSV (Hue, Saturation and Value) color channels. Hence, the algorithm is suitable for defogging along with color correction. Consumer video surveillance systems could inevitably use this algorithm to mitigate the atmospheric artifacts.

A nearly real-time algorithm was developed by Gibson et al., [45] which could operate in fractions of a second. Earlier literatures offered either fog removal or turbulence removal but not both simultaneously. This work succeeded in bringing up a new algorithm namely; Contrast Enhancement and Turbulence Mitigation (CETM) utilized the inference from contrast enhancement to improve the turbulence removal. Further, temporal consistency had been verified with Turbulence Mitigation Metric (TMM).

Filter based approach had been used in [46]. The approach was subdivided into several tasks including depth and color estimation. These estimations were finally used for visibility restoration. Median filter was implemented for depth estimation along with adaptive gamma correction. While doing gamma correction, halo effects were avoided in images with complex structural information. Color analysis module was used to estimate the actual color information of the input blurred image. Though, single image dehazing is tough,, the proposal could perform better color details than the existing state-of-art algorithms

Yet another method found [47], for defogging the image while utilizing single image. Atmospheric scattering model was used from which atmospheric veil was estimated through local extrema method. Tone and contrast were adjusted through multi-scale tone manipulation algorithm. This algorithm could produce better results both by visibility and color information.

Dong et al., researched in [48] in single frame infrared target retrieval under bad weather conditions especially strong ocean waves and sea fog. The respective authors revised the Visual Attention Model (VAM) and integrated with anti-vibration pipeline-filtering algorithm (a multi frame clutter removal method) to detect the weak targets seen on image borders. An automatic extraction of Saliency Map (SM) followed by background clutter suppression could yield better visual experience than the existing results in different weather conditions, especially for maritime targets.

He et al, in [10] could obtain better results without using the ground truth images, by estimating the optimal transmission map from haze image only. In order to re-alter the initial transmission map, difference structure-preservation dictionary was utilized to preserve the vital steady features of the transmission map.

IV. METRICS

Various metrics related to dehazing performance is evaluated under two cases as reported below.

A. Known Ground Truth

1) Mean Square Error

$$MSE = \frac{1}{m \times n} \sum_{i=0}^{m-1} \sum_{j=0}^{n-1} [I(i, j) - K(i, j)]^2 \quad (8)$$

Where, $I(i, j)$ is the gray level of the ground truth image and $K(i, j)$ is the gray level of the haze free image.

2) Peak Signal to Noise Ratio (PSNR)

$$PSNR = 10 \log_{10} \left(\frac{255^2}{MSE} \right) \quad (9)$$

3) Structural Similarity Index metric (SSIM)

$$SSIM(i, j) = \left(\frac{2\mu_i\mu_j + c_1}{\mu_i^2 + \mu_j^2 + c_1} \right) \left(\frac{2\mu_{pq} + c_2}{\sigma_i^2 + \sigma_j^2 + c_2} \right) \quad (10)$$

Where, i, j represents the pixel coordinates. The terms, μ_i, μ_j, σ_i^2 and σ_j^2 are means and variances of i^{th} and j^{th} pixel respectively. Cross-covariance between pixels of i^{th} and j^{th} location is denoted as σ_{ij} . The default values for c_1 and c_2 are 0.01 and 0.03 respectively.

4) Figure of Merit (FOM)

This metric can be used to obtain the edge shifts due to improper reconstruction of the images especially in the encryption and compression domain. FOM is calculated between the original haze free image and the enhanced haze removed image as given in Equation (11).

$$R = \frac{1}{I_n} \sum_{i=1}^{I_A} \frac{1}{1 + \alpha d^2} \quad (11)$$

Where,

$I_n = \max(I_I, I_A)$, I_I = number of ground truth edge points, I_A = number of haze free edge points, d = displacement of haze free edge points from ground truth edge, α = scaling constant

B. Unknown Ground Truth

1) Percentage of saturated pixels

Percentage of saturated pixels (τ) as mentioned in [43] reveals on the quality of image whether the enhanced images are over brightened or over contrasted due to the saturation of pixel values when processed using some algorithms. It is mathematically represented and computed as follows [49]

$$\tau = \frac{S}{m \times n} \quad (12)$$

Where, S denotes the pixel count whose value reaches either 0 or 255 for completely black or white respectively in 8 bit quantized images after the haze removal techniques, which were not present in the input hazy image. The lower value of τ is appreciable for better dehazing performance

2) Visible edges ratio

The ratio of new visible edges (e) and ratio of average gradient (\bar{r}) are also utilized to monitor the dehazing performance. The e represents the improved rate of visible edges of haze free images, and is calculated as given in [50].

$$e = \frac{n_k - n_l}{n_l} \quad (13)$$

Where, the number of vital visible edges in the haze image I are denoted by n_k and that of the haze free image K is represented by n_l . The higher value of e emphasizes the obtained edges are stronger in haze removed images. To calculate \bar{r} , rate of change of edge pixels intensities are used to find the restoration degree of both edges and texture content of the original scene. \bar{r} is depicted as follows:

$$\bar{r} = e^{\left[\frac{1}{n_k} \sum_{i \in \Phi_k} \log r_i \right]} \quad (14)$$

Where, $r_i = \frac{V_k}{V_l}$, V_k and V_l are the gradients of edges k and l respectively, and r_i indicates the overall quality of the set of visible edges of K . A better protection of edges is ensured through the higher values of \bar{r} than the existing methods.

3) Perceptual Haze density

It is essential to know the amount of residual haze still present in the recovered image after dehazing. In [51], haze density prediction is done using several statistical features. The input image divided into blocks of size $M \times M$ and aggregate mean values are computed. Features such as variance, sharpness, contrast energy, image entropy, dark channel prior, color saturation, colorfulness etc are calculated by utilizing all the blocks of size $M \times M$. A distance metric, especially Mahalanobis distance D is applied on the aforementioned features as given below.

$$D = \sqrt{(m_1 - m_2)^t \left(\frac{C_1 + C_2}{2} \right)^{-1} (v_1 - v_2)} \quad (16)$$

where, m_1 and m_2 are mean vectors and C_1 and C_2 are covariance matrices for Multivariate Gaussian (MVG) model of the haze free quantity and MVG fit of the haze image. MVG fit is mathematically calculated as shown below.

$$P(s) = \frac{1}{\sqrt{2\pi n} \text{mod}(D)} \exp(-0.5 \times (s - \mu)^t C^{-1} (s - \mu)) \quad (15)$$

Where, s denotes the statistical features, μ represents mean and $n \times n$ represents the covariance matrix of different hazy features. Also, D represents determinant and C^{-1} depicts the covariance matrix inverse for MVG derived using maximum likelihood (ML) method [53].

The results and performance analysis on dehazing methods from specific literatures have been presented below.

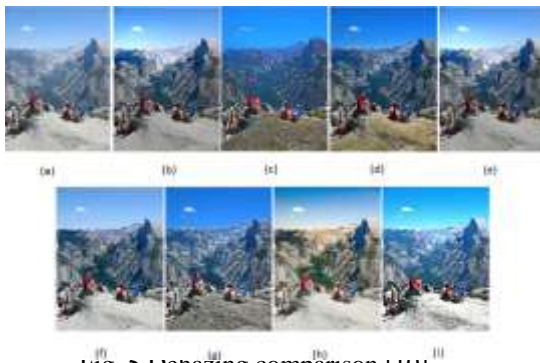


Fig. 5 Dehazing comparison [10]

(a) in figures are displayed, the results of (b)-(i) are obtained [4],[19], [8],[1], [5], [20], [59], [10].

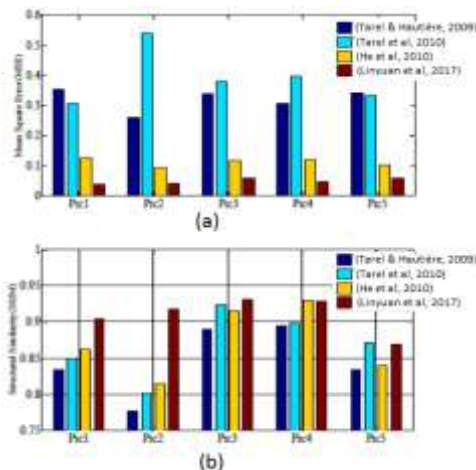


Fig. 6 MSE and SSIM comparison [10]

C. Significance of dehazing Methods

1) Indoor scenes

Images acquired in indoor using drones or images from fixed cameras could yield hazy images due to scattering by indoor lightings. Hence it is vital to enhance the images acquired in common life scenario and domestic functions to capture the life moments with good quality images [54].

2) Outdoor Road, Train and Air traffic scenes

It is always difficult to drive the vehicles in

misty climate especially during the bad weather conditions. Adding the driver assistance systems in automobiles are trending in recent days due to reasonable expectation from the common users for a safety drive. The same scenario is applicable to railways and aviation traffic to avoid train collisions due to haze in vision [55].

3) Underwater scenes

The focal role in ocean engineering is to explore the life under water to access the geological and biological environments. Hence, dehazing under water images would help the related community to obtain relevant benefits [56],[57].

4) Remote sensing

Images acquired from satellites for the purpose of weather forecasting require good attention on extracting the true information in the image [58].

D. Expectations

An ideal expectation from a dehazing algorithm is presented below.

1) Single image: Reference images such as Ground truth images and Multi-temporal images would increase processing time. Hence, Dehazing is required to be done with single image.

2) Fully automatic: The constructed dehazing method should not need any manual inputs or human assistance. Also, manual tuning never to be encouraged in such systems as it would fetch inescapable human errors.

3) Independent from constant values: Mathematical model of dehazing proposals are expected to be free from constants involved in the equations. These constants may not be suitable for all images containing distinct scenes [9].

4) Fast: The processing speed is very critical in case of videos from real time moving scenes. Processing time of 1.52 s to 6.47 s is commonly seen [8], [39], [54]. Time of processing less than 1 s would be highly appreciated.

5) Wide operational range of image intensity, color and size: The system is expected to handle wide range of image sizes as it is directly proportional to the processing time. Dehazing should be robust even when the object intensity or color is matching with the haze pixels.

Table 2. Qualitative comparison of Fig. 5

		[4]	[19]	[8]	[7]	[20]	[18]	[59]	[10]
Building	e	-0.06	-0.14	0.06	0.05	0.07	-0.01	0.04	0.04
	τ	0.09	0.02	0.00	0.00	0.00	0.46	0.00	0.01
	$\bar{\tau}$	1.32	2.34	1.42	1.42	1.88	1.81	1.86	1.73
Landscape	e	0.04	0.08	0.08	0.09	0.02	0.11	0.03	0.05
	τ	0.02	0.01	0.01	0.00	0.00	0.71	0.31	0.15
	$\bar{\tau}$	1.23	2.28	1.33	1.62	2.09	1.79	1.83	1.82
Person	e	0.05	-0.03	0.03	0.05	0.04	-0.12	0.10	0.11
	τ	0.03	0.02	0.01	0.00	0.01	0.41	0.25	0.27
	$\bar{\tau}$	1.15	2.32	1.52	1.52	2.22	2.19	1.93	2.04

V. CONCLUSION AND RECOMMENDATIONS

In this survey, existing model of image degradation due to bad weather has been studied. Various restoration methods have been discussed while pointing both merits and demerits of those methods. It is understood that restoration fully depends on efficient retrieval of depth map and transmission map properly. No method is applicable globally for all types of haze images. Several algorithms could overestimate the restoration model instead the actual ground truth. The specific literatures [59], [60] and [61] have discussed on high speed dehazing constraints. Therefore, computation time of the proposed algorithm is to be compared with aforementioned research works. Most of the works were carried out with simulations and only few works have been tried with real camera based acquisition. It is suggested to conduct the further researches to improve the performance shown in Table 2, based on Statistics and Chaos based Atmospheric unveiling method (SCAUM) which would resemble the following steps.

1. Calculation of Mutual Information, Kurtosis, Skewness, Standard deviation on image scene.
2. Calculation of chaotic parameters namely, Kolmogorov-Sinai Entropy density and Kolmogorov-Sinai Entropy generality.
3. To calculate the atmospheric veil along with corrections based on the external light, light scattering effects and the parameters are used from step 1 and step 2.

Further recommendation is to design unveiling process based on Mutual information and correlation coefficients using Fog identification-Then-Unveiling (FITU). This method is expected to reduce the ambiguity in differentiating the fog pixels and actual objects in the scene. In order to optimize the performance of SCAUM and FITU, fuzzy logic and Differential Evolution (DE) methods may be utilized to reduce the error metrics. Various metrics related to dehazing performance is evaluated under two cases as reported below.

REFERENCES

- [1] Y. J. Kaufman, D. Tanre, H. R. Gordon, T. Nakajima, J. Lenoble, R. Frouin, H. Grassl, B. M. Herman, M.D. King and P. M. Teillet, (1997) "Passive remote sensing of tropospheric aerosol and atmospheric correction for the aerosol effect. *Journal of Geophysical Research: Atmospheres*," vol. 102(D14), no. 16, pp. 815–16,830, 1991.
- [2] S. G. Narasimhan and S. K. Nayar, "Vision and the Atmosphere," *International Journal of Computer Vision*, vol. 48, no. 3, pp. 233-254, 2002.
- [3] H. Yang, P. Chen, C. Huang, Y. Zhuang, and Y. Shiau, "Low Complexity Underwater Image Enhancement Based on Dark Channel Prior". *Proceedings of 2nd International Conference on Innovations in Bio-inspired Computing and Applications*, Shenzhen, 2011, pp. 17-20.
- [4] R. Fattal, "Single image dehazing," *ACM transactions on graphics (TOG)*, vol. 27, no. 3, pp. 1-9, 2008.
- [5] E. J. McCartney, "Optics of the atmosphere: Scattering by molecules and particles", New York, John Wiley and Sons, 1976.
- [6] S. G. Narasimhan and S. K. Nayar, "Contrast Restoration of Weather Degraded Images", *IEEE Transactions on Pattern Analysis and Machine Intelligence*, vol. 25, no. 6, pp. 713-724, 2003.
- [7] J. Kopf, B. Neubert, B. Chen, M. Cohen, D. Cohen-Or, O. Deussen, M. Uyttendaele and D. Lischinski, "Deep photo: Model-based photograph enhancement and viewing", *ACM Trans. on Graphics*, vol 27, no. 5, pp. 32-39, 2008.
- [8] K. He, J. Sun and X. Tang, "Single image haze removal using dark channel prior," *IEEE Transactions on Pattern Analysis and Machine Intelligence*, vol. 33, no. 12, pp. 2341–2353, 2011.
- [9] Q. Zhu, J. Mai, and L. Shao, "A Fast Single Image Haze Removal Algorithm Using Color Attenuation Prior," *IEEE Transactions on Image Processing*, vol. 24, no.11, pp. 3522-3533, 2011.
- [10] L. He, J. Zhao, N. Zheng, and D. Bi, "Haze Removal using the Difference-Structure-Preservation Prior," *IEEE Transactions on Image Processing*, vol. 26, no. 3, pp. 1063-1075, 2017.
- [11] E. J. Candes and D.L. Donoho, "New tight frames of curvelets and optimal representations of objects with piecewise C^2 singularities," *Communications on Pure and Applied Mathematics*, vol. 57, no. 2, pp. 219-266, 2003.
- [12] M. N. Do and M. Vetterli, "The contourlet transform: An efficient directional multi-resolution image representation," *IEEE Transaction on Image Processing*, vol. 14, no. 12, pp. 2091–2106. 2005.
- [13] M. Aharon, M. Elad, and A. Bruckstein, "The K-SVD: An algorithm for designing of over complete dictionaries for sparse representation," *IEEE Transactions on Signal Processing*, vol. 54, no. 11, pp. 4311-4322, 2006.
- [14] M. Elad and M. Aharon, "Image denoising via sparse and representations over learned dictionaries," *Transactions on Image Processing*, vol. 15, no. 12, pp. 3736-3745, 2006.
- [15] K. Dabov, A. Foi, V. Katkovnik and K. Egiazarian, "Image denoising by sparse 3D transform domain collaborative filtering," *IEEE Transactions on Image Processing*, vol. 16, no. 8, pp. 2080-2095, 2007.
- [16] P. Chatterjee and P. Milanfar, "Clustering-based denoising with locally learned dictionaries", *IEEE Transactions on Image Processing*, vol. 18, no. 7, pp. 1438-1451, 2009.
- [17] L. Li, W. Feng and J. Zhang, "Contrast enhancement based single image dehazing via TV-L1 minimization," *IEEE International Conference on Multimedia and Expo (ICME)*, Chengdu, 2014, pp. 1-6, 2014.
- [18] K. Nishino, L. Kratz and S. Lombardi, "Bayesian Defogging," *International Journal of Computer Vision*, vol. 98: 263, 2012.
- [19] R. T. Tan, "Visibility in bad weather from a single image," *Proceedings of IEEE Conference on Computer Vision and Pattern Recognition*, Anchorage, Alaska, USA, pp. 1–8, 2008.
- [20] L. Caraffa and J. Tarel, "Markov Random Field Model for Single Image Defogging," *IEEE Intelligent Vehicles Symposium (IV)*, Gold Coast, QLD, pp. 994-999, 2013.
- [21] Y. Wang and C. Fan, "Single Image Defogging by Multiscale Depth Fusion," *IEEE Transactions on Image Processing*, vol. 23, no. 11, pp. 4826–4837, 2014.
- [22] K. He, J. Sun and X. Tang, "Guided image filtering," *Proc. European Conference on Computer Vision*, Crete, Greece, pp. 1-14, 2010.
- [23] B. Xie, F. Guo and Z. Cai, "Improved Single Image Dehazing Using Dark Channel Prior and Multi-scale Retinex," *Proceedings of International Conference on Intelligent System Design and Engineering Application*, Changsha, 2010, pp. 848-851, 2010.

- [24] H. Xu, J. Guo, Q. Liu and L. Ye, "Fast image dehazing using improved dark channel prior," Proceedings of IEEE International Conference on Information Science and Technology, Hubei, 2012, pp. 663-667, 2012.
- [25] Y. Lai, Y. Chen and C. Hsu, "Single Image Dehazing With Optimal Transmission Map," Proceedings of the 21st International Conference on Pattern Recognition (ICPR2012), Tsukuba, 2012, pp. 388-391, 2012.
- [26] G. Meng, Y. Wang, J. Duan, S. Xiang and C. Pan, "Efficient image dehazing with boundary constraint and contextual regularization," IEEE International Conference on Computer Vision, Sydney, NSW, 2013, pp. 617-624, 2013.
- [27] F. C. Cheng, C. H. Lin and J. L. Lin, "Constant time $O(1)$ image fog removal using lowest level channel," Electronics Letters, vol. 48, no. 22, pp. 1404-1406, 2012..
- [28] D. Pomerleau, "Visibility estimation from a moving vehicle using the RALPH vision system," Proceedings of Conference on Intelligent Transportation Systems, Boston, MA, USA, 1997, pp. 906-911, 1997.
- [29] N. Hautiere, R. Labayrade and D. Aubert, "Real-time disparity contrast combination for onboard estimation of the visibility distance," IEEE Transactions on Intelligent Transportation Systems, vol. 7, no. 2, pp. 201-212, 2006.
- [30] N. Hautiere, J. Tarel, D. Aubert and E. Dumont, "Blind contrast enhancement assessment by gradient ratioing at visible edges," Image Analysis & Stereology, vol. 27, no. 2, pp. 87-95, 2011.
- [31] K. Mori, T. Takahashi, I. Ide, H. Murase, T. Miyahara and Y. Tamatsu, "Recognition of foggy conditions by in-vehicle camera and millimeter wave radar," Proceedings of IEEE Intelligent Vehicles Symposium, Istanbul, 2007, pp. 87-92, 2007.
- [32] C. Boussard, N. Hautiere and B. d'Andréa Novel, "Vehicle dynamics estimation for camera-based visibility range estimation," IEEE/RSJ International Conference on Intelligent Robots and Systems, Nice, 2008, pp. 600-605, 2008.
- [33] L. L. Grewe and R. R. Brooks, "Atmospheric Attenuation Reduction through Multisensor Fusion," Proceedings of SPIE, Sensor Fusion: Architectures, Algorithms, and Applications II, vol. 3376, 1998.
- [34] S. G. Narasimhan and S. K. Nayar, "Vision in Bad Weather," Proceedings of the Seventh IEEE International Conference on Computer Vision, Kerkyra, Greece, 1999, pp. 820-827 vol.2, 1999.
- [35] S. G. Narasimhan and S. K. Nayar, "Chromatic Framework for Vision in Bad Weather," Proceedings of IEEE Conference on Computer Vision and Pattern Recognition. CVPR 2000 (Cat. No.PR00662), Hilton Head Island, SC, 2000, pp. 598-605 vol.1, 2000.
- [36] Narasimhan, S.G., Nayar, S.K. (2002) "Vision and the Atmosphere," International Journal of Computer Vision, 48(3): pp. 233-254.
- [37] S. G. Narasimhan and S. K. Nayar, "Contrast Restoration of Weather Degraded Images," IEEE Transactions on Pattern Analysis and Machine Intelligence, vol. 25, no. 6, pp. 713-724, 2003.
- [38] N. Hautiere, J. Tarel and D. Aubert, "Towards fog-free in-vehicle vision systems through contrast restoration," Proceedings of IEEE Conference on Computer Vision and Pattern Recognition, Minneapolis, MN, 2007, pp. 1-8, 2007..
- [39] J. Tarel and N. Hautière, "Fast visibility restoration from a single color or gray level image," Proceedings of IEEE International Conference on Computer Vision (ICCV'09), Kyoto, Japan, 2009, pp. 2201-2208, 2009.
- [40] N. Hautiere, J. Tarel and D. Aubert, "Mitigation of Visibility Loss for Advanced Camera-Based Driver Assistance," IEEE Transactions On Intelligent Transportation Systems, vol. 11, no. 2, pp. 474-484, 2010..
- [41] A. K. Tripathi and S. Mukhopadhyay, "Single image fog removal using anisotropic diffusion," IET Image Processing, vol. 6, no. 7, pp. 966-975, 2012.
- [42] P. Perona and J. Malik, "Scale-space and edge detection using anisotropic diffusion," IEEE Transactions on Pattern Analysis and Machine Intelligence, vol. 12, no. 7, pp. 629-639, 1990.
- [43] A. K. Tripathi and S. Mukhopadhyay, "Removal of Fog from Images: A Review," IETE Technical Review, vol. 29, no. 2, pp. 148-156, 2012.
- [44] I. Yoon, S. Kim, D. Kim, M. H. Hayes and J. Paik, "Adaptive Defogging with Color Correction in the HSV Color Space, for Consumer Video Surveillance System," IEEE Transactions on Consumer Electronics, vol. 58, no. 1, pp.111-116, 2012.
- [45] K. B. Gibson and T. Q. Nguyen, "An Analysis and Method for Contrast, Enhancement Turbulence Mitigation", IEEE Transactions on Image Processing, vol. 23, no. 7, pp. 3179-3190, 2014.
- [46] S. Huang, B. Chen and W. Wang, "Visibility Restoration of Single Hazy Images Captured in Real-World Weather Conditions," IEEE Transactions on Circuits and Systems for Video Technology, vol. 24, no. 10, pp. 1814-1824, 2014.
- [47] H. Zhao, C. Xiao, J. Yu and X. Xu, "Single Image Fog Removal Based on Local Extrema," IEEE/CAA Journal Of Automatica Sinica, vol. 2, no. 2, pp-158- 165, 2015.
- [48] L. Dong, B. Wang, M. Zhao, and W. Xu, "Robust Infrared Maritime Target Detection Based on Visual Attention and Spatiotemporal Filtering," IEEE Transactions on Geoscience and Remote Sensing, vol. 55, no. 5, pp. 3037-3050, 2017..
- [49] D. Singh and V. Kumar, "Dehazing of remote sensing images using improved restoration model based dark channel prior," The Imaging Science Journal, vol. 65, no. 5, pp. 282-292, 2017.
- [50] N. Hautiere, J. Tarel, D. Aubert, and E. Dumont, "Blind contrast enhancement assessment by gradient ratioing at visible edges", Image Analysis & Stereology, vol. 27, no. 2, pp. 87-95, 2011.
- [51] L. K. Choi, J. You, A. C. Bovik, "Referenceless prediction of perceptual fog density and perceptual image defogging", IEEE Transactions on Image Processing, vol. 24, no. 11, pp. 3888-3901, 2015.
- [52] J. M. Valls, R. Aler, O. Fernandez, "Using a mahalanobis-like distance to train radial basis neural networks. In: Cabestany J, Prieto A, Sandoval F (eds) Computational Intelligence and Bioinspired systems". IWANN 2005, Lecture Notes in Computer Science, vol 3512. Springer, Berlin, Heidelberg, 2005.
- [53] R. O. Duda, P. E. Hart, and D. G. Stork, "Pattern classification". Wiley, New York, 2012.
- [54] K. Kim, S. Kim and K. S. Kim, "Effective image enhancement techniques for fog-affected indoor and outdoor images", IET Image Process., vol. 12, no. 4, pp-465-471, 2018.
- [55] S. C. Huang, B. H. Chen BH and Y. J. Cheng, "An efficient visibility enhancement algorithm for road scenes captured by intelligent transportation systems," IEEE Trans Intell Transp Syst, vol. 15, no. 5, pp. 2321-2332, 2014.
- [56] S. Serikawa and H. Lu, "Underwater image dehazing using joint trilateral filter," Comput Electr Eng, vol. 40, no.1, pp. 41-50, 2014.
- [57] J. Y. Chiang and Ying-Ching Chen, "Underwater Image Enhancement by Wavelength Compensation and Dehazing," IEEE Transactions On Image Processing, vol. 21, no. 4, pp. 1756-1769, 2012.
- [58] X. Pan, F. Xie, Z. Jiang and J. Yin, "Haze removal for a single remote sensing image based on deformed haze imaging model," IEEE Signal Processing Letters, vol. 22, no. 10, pp.1806-1810, 2015

- [59] R. Fattal, “*Dehazing using Color line*”, ACM Trans. Graph, vol. 34, no. 1, pp. 256-269, 2014.
- [60] D. Singh and V. Kumar, “*Modified gain intervention filter based dehazing technique*,” Journal of Modern Optics, vol. 64, no. 20, pp. 2165-2178, 2017.
- [61] S. Salazar-Colores, I. Cruz-Aceves and J.M.Ramos-Arreguin, “*Single image dehazing using a multilayer perceptron*”, Journal of Electronic Imaging, vol. 27, no. 4, 2018.
- [62] http://web.cse.ohio-state.edu/~parent.1/classes/782/Lectures/03_Radiometry.pdf
- [63] Coakley, J. A. (2003). J. R. Holton and J. A. Curry, eds. “*Reflectance and albedo, surface*” (PDF). Encyclopedia of the Atmosphere. Academic Press. pp. 1914–23.